International Journal of Heat and Mass Transfer 52 (2009) 5776–5783

Contents lists available at ScienceDirect

International Journal of Heat and Mass Transfer

journal homepage: www.elsevier.com/locate/ijhmt

Critical times in multilayer diffusion. Part 1: Exact solutions

R.I. Hickson [a], S.I. Barry [a,b,*], G.N. Mercer [b]

[a] School of Physical, Environmental and Mathematical Sciences, University of New South Wales at ADFA, Northcott Drive, Canberra, ACT 2600, Australia
[b] National Centre for Epidemiology and Public Health, Australian National University, Canberra, ACT 0200, Australia

ARTICLE INFO

Article history:
Received 1 April 2009
Received in revised form 17 August 2009
Available online 18 September 2009

Keywords:
Diffusion
Multilayer
Critical time
Time lag
Laminates
Composite materials

ABSTRACT

While diffusion has been well studied, diffusion across multiple layers, each with different properties, has had less attention. This type of diffusion may arise in heat transport across composite materials or layered biological material. Usually of most interest is a critical time, such as the time for a material to heat up. Here an exact solution is found which is used to numerically demonstrate the critical time behaviour for transport across multiple layers with imperfect contact. This solution illustrates the limitations of traditional averaging methods, which are only good for a large number of layers.

1. Introduction

Diffusion through multiple layers has applications to a wide range of areas in heat and mass transport. Industrial applications include annealing steel coils [1–3], the performance of semiconductors [4] and electrodes [5,6], and geological profiles [7]. Biological applications include determining the effectiveness of drug carriers inserted into living tissue [8], the probing of biological tissue with infrared light [9], and analysing the heat production of muscle [10].

For multilayer diffusion across n layers the standard diffusion equation,

$$\frac{\partial U_i}{\partial t} = D_i \frac{\partial^2 U_i}{\partial x^2}, \quad i \in [1, n], \tag{1}$$

is applicable in each layer where $x_{i-1} \leqslant x \leqslant x_i$ is distance, U_i is the temperature in layer i at time t, and D_i is the diffusivity of layer i, as shown in Fig. 1. For clarity, in subsequent sections the notation $d_i \equiv \sqrt{D_i}$ is also used.

Exact solutions for diffusion in layered media have been found for diverse applications and geometries. These include solutions in Cartesian coordinates for two layers [8,11,12] and n layers [13–17], and cylindrical n layer solutions [18,19]. Many of the publications use mathematical separation methods similar to that outlined in Sections 2 and 3 of this article. However, previous publications that use separation methods, and also consider Cartesian coordinates, assume perfect contact between the layers [13–17] and some [13,14,17] have less general boundary conditions. Laplace transform approaches are also used [5,20], but are less common due to the difficulty of the inverse transforms, which are often only numerically found.

An important aspect of multilayer diffusion is the 'critical time', which is a measure of how long the diffusive process takes. There are multiple definitions of critical time since mathematically, an infinite amount of time is required to reach steady state [21]. One definition, appropriate in the annealing of steel coils [1–3], is when the coldest point in the coil reaches a given temperature. A common and more general definition we consider here is the time when the average temperature reaches a given or specified proportion of the average steady state. That is, the value of $t = t_c$ such that

$$\int_{x=0}^{L} U(x, t_c)dx = \alpha \int_{x=0}^{L} w(x)dx, \tag{2}$$

where $U(x, t)$ is the temperature, $0 < \alpha < 1$ is a chosen constant, and $w(x)$ is the steady state. Landman and McGuinness [21] summarise previous work and applications using this critical time definition, also called the mean action time [22,23].

The most common approximation of critical time (see for example [24–28]), is the simple expression

$$t_{av} = \frac{L^2}{6D_{av}}, \tag{3}$$

* Corresponding author. Address: National Centre for Epidemiology and Public Health, Australian National University, Canberra, ACT 0200, Australia. Tel.: +61 2 6125 9506; fax: +61 6125 0740.
E-mail addresses: R.I.Hickson@gmail.com (R.I. Hickson), Steven.Barry@anu.edu.au (S.I. Barry).

0017-9310/$ - see front matter © 2009 Elsevier Ltd. All rights reserved.
doi:10.1016/j.ijheatmasstransfer.2009.08.013

Nomenclature

c_i	layer specific heat
$D = d^2$	single layer diffusivity
$D_{av} = d_{av}^2$	average diffusivity
$D_i = d_i^2$	layer diffusivity
$f(x)$	initial condition
L	total length of medium
l_i	layer width
H_i	contact transfer coefficient
n	total number of layers
t	time
t_{av}	typical critical time
t_c	multilayer critical time
t_s	single layer critical time
$U(x,t)$	temperature
$v(x,t)$	transient solution
$w(x)$	steady state solution

Additional notation

$[A,B]$	shorthand for $n/2$ biperiodic layers, material properties D_A, D_B as $ABAB\ldots AB$
x	spatial position

Greek symbols

α	proportion of the steady state
κ_{av}	average conductivity
κ_i	layer conductivity
λ_m	multilayer eigenvalues
μ_m	single layer eigenvalues
ρ_i	layer density
θ_1	boundary condition at $x = x_0$
θ_2	boundary condition at $x = x_n$

Subscripts

i	layer index
m	eigenvalue index

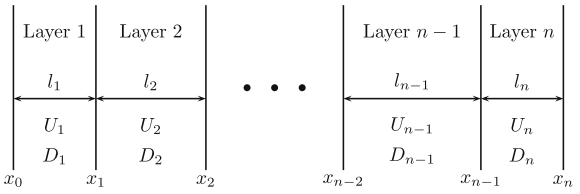

Fig. 1. Multilayer schematic showing the nomenclature. Here U_i is the temperature in layer i at time t, D_i is the diffusivity of a given layer and l_i is the width of the layer.

where D_{av} is the commonly averaged diffusivity for layered materials, given by

$$\frac{L}{D_{av}} = \sum_{i=1}^{n} \frac{l_i}{D_i}. \tag{4}$$

Here L is the total medium length, and l_i are the lengths of each layer with material diffusivity D_i. This series-averaged diffusivity is a valid measure when calculating heat fluxes at steady state, or for a large number of layers. The critical time, Eq. (3), is found using the exact solution for the one layer problem, with different surface concentrations [26]. The flux, Q_t, is calculated at $x = x_0$ and integrated over time. The asymptotic line is found, as $t \to \infty$, and is rearranged for t when $Q_t = 0$. See Crank [26, pp. 47–48], for a more detailed explanation. Eq. (3) corresponds to the critical time definition given in Eq. (2) for $\alpha \approx 0.8435$, a result calculated in Section 2. Here α corresponds to the asymptotic analysis conducted by Crank [26] to quantify a 'breakthrough' or 'lag' time. However, Eq. (3) is only strictly valid for a single layer of material. Absi et al. [29] describe a brief numerical and experimental comparison using Eq. (3) versus the full coupled numerical system for two layers. Their results indicate the limitations of this formula, a result we corroborate in our numerical simulation shown in Fig. 3.

Several publications have attempted to calculate a diffusive critical time through composites, in Cartesian, cylindrical and spherical geometries with Ash et al. [24,30] giving detailed solutions. These are summarised in Barrer [25] for some of the usual layer configurations, such as two repeated layers, $ABAB\ldots$, also referred to as a 'biperiodic region'. Their complicated derivation is equivalent to choosing $\alpha \approx 0.8435$ in Eq. (2). However, as discussed in detail in our companion paper [31], their result is only as accurate as the approximate result given by Eq. (3), that is of the order of 10–50%. Aguirre et al. [4] determined a solution for sinusoidally imposed temperature, calculating an effective diffusivity for a composite material. Their result is an improved version of the series-averaged diffusivity given in Eq. (4). The effective diffusivity was found in terms of the imposed frequency where Eq. (4) is reflected in the low frequency limit when the material is in quasi-steady state.

Previous work [14] explored a different definition of critical time, where the temperature at the end of the region reached a critical threshold. This definition is only applicable for an insulated boundary condition, whereas a more general definition which is not dependent on the boundary conditions is now considered. Also, we consider here the more general case of imperfect contact between the layers.

We will show standard Eqs. (3) and (4) give inaccurate results. The exact solution is found for diffusion in a one-dimensional Cartesian material with only one layer in Section 2. This is extended to the more complicated multilayer case in Section 3 where the solutions are also verified. The critical time is calculated numerically in Section 4 and discussed in Section 5.

2. Single layer solution

In this section we find an exact solution for the single layer case. Whilst not original (see for example [32]), this will demonstrate the solution method used for the more difficult multilayer diffusion problem in Section 3. Additionally, these results will assist in understanding the definition and behaviour of critical time.

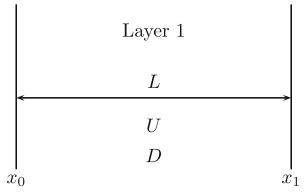

Fig. 2. Single layer diffusion for $U(x,t)$, length L, and a single diffusivity, D.

The single layer case is depicted in Fig. 2, where

$$\frac{\partial U}{\partial t} = D\frac{\partial^2 U}{\partial x^2}, \tag{5}$$

for some initial condition, $U(x,0) = f(x)$, and mixed boundary conditions,

$$\begin{aligned} a_1 U + b_1 \frac{\partial U}{\partial x} &= \theta_1 \qquad \text{at} \quad x = x_0, \\ a_2 U + b_2 \frac{\partial U}{\partial x} &= \theta_2 \qquad \text{at} \quad x = x_1, \end{aligned} \tag{6}$$

where $a_1, a_2, b_1, b_2, \theta_1$ and θ_2 are constants.

Due to the boundary conditions the problem must be split into the steady state, $w(x)$, and transient, $v(x,t)$, components [32] where $U(x,t) = w(x) + v(x,t)$. The steady state solution is found by integrating and substituting in the boundary conditions to give

$$w(x) = \frac{(a_1\theta_2 - a_2\theta_1)(x - x_0) + \theta_1(a_2 L + b_2) - b_1\theta_2}{a_1 a_2 L + a_1 b_2 - a_2 b_1}. \tag{7}$$

It has been assumed that a_1 and a_2 cannot both be zero. If $a_1 = 0 = a_2$ then a solution only exists if $b_2\theta_1 = b_1\theta_2$; otherwise the finite medium has an unbalanced heat input giving rise to unbounded temperature.

The transient solution, $v(x,t)$, satisfies

$$\frac{\partial v}{\partial t} = D\frac{\partial^2 v}{\partial x^2}, \tag{8}$$

$$a_1 v + b_1 \frac{\partial v}{\partial x} = 0 \qquad \text{at} \quad x = x_0, \tag{9}$$

$$a_2 v + b_2 \frac{\partial v}{\partial x} = 0 \qquad \text{at} \quad x = x_1, \tag{10}$$

$$v(x,0) = g(x), \tag{11}$$

where $g(x) = f(x) - w(x)$. This can be solved using separation of variables where $v(x,t) = X(x)T(t)$, resulting in

$$T(t) = e^{-\mu_m^2 t}, \tag{12}$$

and the eigenfunction solutions

$$X_m(x) = \sin\left(\frac{\mu_m}{d}(x - x_0)\right) - \frac{b_1\mu_m}{a_1 d}\cos\left(\frac{\mu_m}{d}(x - x_0)\right), \tag{13}$$

where we use the simpler notation $d = \sqrt{D}$ and the eigenvalues, μ_m, satisfy

$$\sin\left(\frac{\mu_m L}{d}\right)\left[\frac{a_1 a_2 d}{\mu_m} + \frac{b_1 b_2 \mu_m}{d}\right] + \cos\left(\frac{\mu_m L}{d}\right)[a_1 b_2 - a_2 b_1] = 0. \tag{14}$$

Therefore the transient solution is

$$v(x,t) = \sum_{m=1}^{\infty} A_m e^{-\mu_m^2 t} X_m(x), \tag{15}$$

where A_m is determined by Sturm–Liouville theory as

$$A_m = \frac{\int_{x_0}^{x_1} g(x) X_m(x)\,dx}{\int_{x_0}^{x_1} X_m^2(x)\,dx}. \tag{16}$$

Hence the complete solution is

$$U(x,t) = w(x) + \sum_{m=1}^{\infty} A_m e^{-\mu_m^2 t} X_m(x). \tag{17}$$

Eq. (2) can now be written as

$$(1-\alpha)\int_{x=x_0}^{x_1} w(x)\,dx + \int_{x=x_0}^{x_1} v(x,t_s)\,dx = 0, \tag{18}$$

for a given critical time, $t = t_s$.

For illustrative purposes we consider the simpler case of constant boundary conditions, where $a_1 = 1 = a_2$ and $b_1 = 0 = b_2$ in Eq. (6). These give $\mu_m = m\pi d/L$ and when $f(x) = 0, A_m = 2(\theta_2(-1)^m - \theta_1)/(m\pi)$. The critical time is then evaluated using Eqs. (17) and (18) to give

$$(1-\alpha)(\theta_1 + \theta_2) + 4\sum_{m=1}^{\infty} \frac{[1 + (-1)^{m+1}]}{(m\pi)^2}\left[\theta_2(-1)^m - \theta_1\right] e^{-\mu_m^2 t_s} = 0. \tag{19}$$

Due to the infinite sum over the eigenvalues, Eq. (19) cannot explicitly be solved for the critical time, t_s. However for large enough times this solution is dominated by the leading order eigenvalue. Hence, if only the leading eigenvalue is considered, when $m = 1$, Eq. (19) can be rearranged to give

$$t_s \approx \frac{L^2}{\pi^2 D}\log\left\{\frac{8}{\pi^2(1-\alpha)}\right\}. \tag{20}$$

Here log refers to the natural logarithm, $\log_e$, to avoid confusion with later notation. The critical time must be positive, therefore $(1 - 8/\pi^2) < \alpha < 1$. Equating this to Eq. (3) gives $\alpha = 1 - (8/\pi^2)\exp(-\pi^2/6) \approx 0.8435$.

Similarly, for an insulated boundary at $x = x_1$, where $a_1 = 1, a_2 = 0, b_1 = 0, b_2 = 1$ and $\theta_2 = 0$ in Eq. (6), the critical time for the leading eigenvalue is

$$t_s \approx \frac{4L^2}{\pi^2 D}\log\left\{\frac{8}{\pi^2(1-\alpha)}\right\}. \tag{21}$$

Equating this to Eq. (3) gives $\alpha = 1 - (8/\pi^2)\exp(-\pi^2/24) \approx 0.4627$. The difference between Eqs. (20) and (21) is of interest, as it shows the insulated case reaches the critical temperature four times more slowly than the non-insulated case. This is a direct consequence of the chosen definition of critical time, since the insulated case has a much higher steady state temperature to reach.

3. Multilayer solutions

In this section the multilayer solution for general boundary conditions are found using the same method as the single layer, by splitting the solution into the steady state, $w_i(x)$, and transient, $v_i(x,t)$, components.

In many situations the contact between layers is imperfect giving rise to a jump condition in U:

$$\kappa_i \frac{\partial U_i}{\partial x} = H_i(U_{i+1} - U_i), \tag{22}$$

$$\kappa_{i+1} \frac{\partial U_{i+1}}{\partial x} = H_i(U_{i+1} - U_i), \tag{23}$$

at $x = x_i$ for $i = 1, 2, \ldots, (n-1)$ where H_i is the contact transfer coefficient and $\kappa_i = D_i\rho_i c_i$ is the conductivity, ρ_i is the density and c_i is the specific heat of layer i. The imperfect contact is depicted in Fig. 3 using temperature profiles, clearly demonstrating the 'jump' at the interfaces. This reflects roughness [1] and contact resistance [32]. If $H_i \to \infty$ then contact becomes perfect and hence this limit represents the equivalent matching conditions

$$U_i(x_i,t) = U_{i+1}(x_i,t), \tag{24}$$

$$\kappa_i \left.\frac{\partial U_i}{\partial x}\right|_{x_i} = \kappa_{i+1} \left.\frac{\partial U_{i+1}}{\partial x}\right|_{x_i}, \tag{25}$$

which represent continuity in 'temperature' and flux, respectively. For Eq. (3) to still be valid for the case of imperfect contact, Eq. (4) must be extended to include the contact resistance, such that

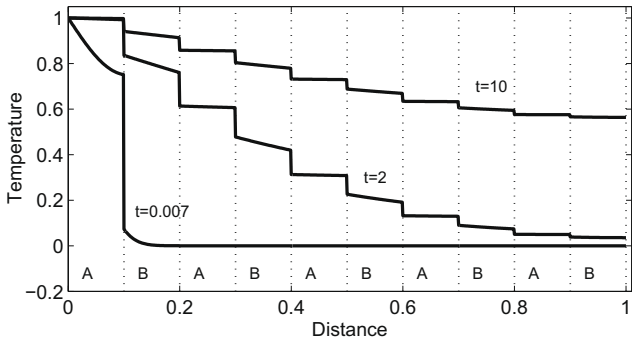

Fig. 3. Temperature profile for a biperiodic region, [1,0.1], with $n = 10, a_1 = 1, b_1 = 0, \theta_1 = 1, a_2 = 0, b_2 = 1, \theta_2 = 0, l_i = 0.1$, and $H_i = 0.5$, at times $t = 0.007, 2, 10$.

$$\frac{L}{D_{\text{av}}} = \sum_{i=1}^{n} \frac{l_i}{D_i} + \sum_{i=1}^{n-1} \frac{1}{H_i}. \tag{26}$$

As $H_i \to \infty$, Eq. (26) approaches Eq. (4).

After Eq. (1) has been split into steady state and transient parts, the steady state solution, $w_i(x)$, satisfies

$$D_i \frac{\partial^2 w_i}{\partial x^2} = 0, \tag{27}$$

$$a_1 w_1 + b_1 \frac{\partial w_1}{\partial x} = \theta_1 \qquad \text{at} \quad x = x_0, \tag{28}$$

$$a_2 w_n + b_2 \frac{\partial w_n}{\partial x} = \theta_2 \qquad \text{at} \quad x = x_n, \tag{29}$$

$$\kappa_i \frac{\partial w_i}{\partial x} = H_i(w_{i+1} - w_i), \tag{30}$$

$$\kappa_{i+1} \frac{\partial w_{i+1}}{\partial x} = H_i(w_{i+1} - w_i). \tag{31}$$

Integrating Eq. (27) results in

$$w_i(x) = q_i(x - x_{i-1}) + h_i, \tag{32}$$

where q_i and h_i are constants. Using the boundary conditions, Eqs. (28) and (29), respectively give

$$h_1 = \frac{\theta_1 - b_1 q_1}{a_1},$$
$$(a_2 l_n + b_2) q_n + a_2 h_n = \theta_2, \tag{33}$$

and the interface conditions, Eqs. (30) and (31), result in recursively defined constants:

$$q_{i+1} = \frac{\kappa_i}{\kappa_{i+1}} q_i = \frac{\kappa_1}{\kappa_{i+1}} q_1, \tag{34}$$

$$h_{i+1} = h_i + q_i\left(\frac{\kappa_i}{H_i} + l_i\right) = h_1 + \sum_{j=1}^{i}\left(\frac{\kappa_j}{H_j} + l_j\right) q_j. \tag{35}$$

These are used to calculate q_n and h_n, which are substituted back into Eq. (33) to find q_1. After some algebra,

$$q_1 = \frac{\kappa_n(a_1\theta_2 - a_2\theta_1)}{a_1 b_2 \kappa_1 - a_2 b_1 \kappa_n + a_1 a_2 \kappa_1 \kappa_n\left(\frac{L}{\kappa_{\text{av}}} + \sum_{j=1}^{n-1} \frac{1}{H_j}\right)}, \tag{36}$$

where

$$\frac{L}{\kappa_{\text{av}}} = \sum_{i=1}^{n} \frac{l_i}{\kappa_i}. \tag{37}$$

Furthermore,

$$q_i = \frac{\kappa_1}{\kappa_i} q_1, \tag{38}$$

$$h_i = h_1 + \kappa_1 q_1 \sum_{j=1}^{i-1}\left(\frac{l_j}{\kappa_j} + \frac{1}{H_j}\right). \tag{39}$$

The inclusion of κ_{av} in Eq. (36) is interesting as it shows averaging of the material properties.

The transient solution, $v_i(x,t)$, satisfies

$$\frac{\partial v_i}{\partial t} = D_i \frac{\partial^2 v_i}{\partial x^2}, \tag{40}$$

$$a_1 v_1 + b_1 \frac{\partial v_1}{\partial x} = 0 \qquad \text{at} \quad x = x_0, \tag{41}$$

$$a_2 v_n + b_2 \frac{\partial v_n}{\partial x} = 0 \qquad \text{at} \quad x = x_n, \tag{42}$$

$$\kappa_i \frac{\partial v_i}{\partial x} = H_i(v_{i+1} - v_i), \tag{43}$$

$$\kappa_{i+1} \frac{\partial v_{i+1}}{\partial x} = H_i(v_{i+1} - v_i). \tag{44}$$

$$v_i(x,0) = f_i(x) - w_i(x) = g_i(x). \tag{45}$$

Using separation of variables, where $v_i(x,t) = X_i(x)T(t)$, results in

$$T(t) = e^{-\lambda_m^2 t}, \tag{46}$$

and the eigenfunction solutions

$$X_{i,m}(x) = J_{i,m} \sin\left(\frac{\lambda_m}{d_i}(x - x_{i-1})\right) + K_{i,m} \cos\left(\frac{\lambda_m}{d_i}(x - x_{i-1})\right), \tag{47}$$

where $J_{i,m}$ and $K_{i,m}$ are constants and λ_m are the eigenvalues. Applying the boundary and interface conditions to Eq. (47) results in a series of expressions that can be rewritten in terms of one of the constants, chosen here as $J_{1,m}$. Hence in Eq. (47), $J_{1,m}$ has been chosen to equal one by normalisation of the eigenfunction. From Eq. (41)

$$K_{1,m} = \frac{-b_1 \lambda_m}{a_1 d_1}, \tag{48}$$

from Eq. (44)

$$J_{i+1,m} = \frac{\kappa_i d_{i+1}}{\kappa_{i+1} d_i}\left[J_{i,m} \cos\left(\lambda_m \frac{l_i}{d_i}\right) - K_{i,m} \sin\left(\lambda_m \frac{l_i}{d_i}\right)\right], \tag{49}$$

and from Eq. (43)

$$K_{i+1,m} = J_{i,m}\left[\sin\left(\lambda_m \frac{l_i}{d_i}\right) + \frac{\kappa_i \lambda_m}{d_i H_i} \cos\left(\lambda_m \frac{l_i}{d_i}\right)\right] + K_{i,m}\left[\frac{-\kappa_i \lambda_m}{d_i H_i} \sin\left(\lambda_m \frac{l_i}{d_i}\right) + \cos\left(\lambda_m \frac{l_i}{d_i}\right)\right]. \tag{50}$$

The eigenvalues, λ_m, are defined by the transcendental expression

$$J_{n,m}\left[a_2 \sin\left(\lambda_m \frac{l_n}{d_n}\right) + \frac{\lambda_m b_2}{d_n} \cos\left(\lambda_m \frac{l_n}{d_n}\right)\right] + K_{n,m}\left[-\frac{\lambda_m b_2}{d_n} \sin\left(\lambda_m \frac{l_n}{d_n}\right) + a_2 \cos\left(\lambda_m \frac{l_n}{d_n}\right)\right] = 0, \tag{51}$$

which comes from Eq. (42). Note $J_{i,m}$ and $K_{i,m}$ are recursively defined.

The transient solution is then

$$v_i(x,t) = \sum_{m=1}^{\infty} C_m e^{-\lambda_m^2 t} X_{i,m}(x). \tag{52}$$

Using the initial condition,

$$v_i(x,0) = g_i(x) = \sum_{m=1}^{\infty} C_m X_{i,m}(x), \tag{53}$$

to solve for the summation constant, C_m, a suitable orthogonality condition must be used. The following orthogonality condition is proven in Appendix A.1,

$$\sum_{i=1}^{n} \rho_i c_i \int_{x_{i-1}}^{x_i} X_{i,m}(x) X_{i,p}(x) dx = \begin{cases} 0, m \neq p \\ \varsigma, m = p \end{cases} \tag{54}$$

where ς is a constant. Using this gives

$$C_m = \frac{\sum_{i=1}^{n} \rho_i c_i \int_{x_{i-1}}^{x_i} g_i(x) X_{i,m}(x)dx}{\sum_{i=1}^{n} \rho_i c_i \int_{x_{i-1}}^{x_i} X_{i,m}^2(x)dx}. \quad (55)$$

The complete solution is therefore

$$U_i(x,t) = w_i(x) + \sum_{m=1}^{\infty} C_m e^{-\lambda_m^2 t} X_{i,m}(x), \quad (56)$$

and has the same form as Eq. (17).

We will now investigate the case of $H_i \to \infty$; when the jump interface solution approaches the matching interface solution. First consider the steady state coefficients, Eqs. (36) and (39). As $H_i \to \infty$,

$$q_1 = \frac{\kappa_n(a_1\theta_2 - a_2\theta_1)}{a_1 b_2 \kappa_1 - a_2 b_1 \kappa_n + a_1 a_2 \kappa_1 \kappa_n \left(\frac{L}{\kappa_{av}}\right)} \quad (57)$$

and

$$h_i = h_1 + \kappa_1 q_1 \sum_{j=1}^{i-1} \frac{l_j}{D_j}. \quad (58)$$

The only equation involving the jump for the transient solution is Eq. (50). As $H_i \to \infty$,

$$K_{i+1,m} = J_{i,m} \sin\left(\lambda_m \frac{l_i}{d_i}\right) + K_{i,m} \cos\left(\lambda_m \frac{l_i}{d_i}\right). \quad (59)$$

The critical time for multiple layers, t_c, is found by solving the equivalent multilayer version of Eq. (18):

$$(1-\alpha) \sum_{i=1}^{n} \int_{x_{i-1}}^{x_i} w_i(x)dx + \sum_{i=1}^{n} \int_{x_{i-1}}^{x_i} v_i(x,t_c)dx = 0. \quad (60)$$

Substituting the solutions from Eqs. (32), (47) and (52) then gives

$$(1-\alpha) \sum_{i=1}^{n} \left\{ h_i l_i + \frac{q_i l_i^2}{2} \right\} + \sum_{i=1}^{n} d_i \sum_{m=1}^{\infty} \frac{C_m}{\lambda_m} e^{-\lambda_m^2 t_c} \Psi_{i,m} = 0, \quad (61)$$

where

$$\Psi_{i,m} = J_{i,m} \left\{ 1 - \cos\left(\frac{\lambda_m l_i}{d_i}\right) \right\} + K_{i,m} \sin\left(\frac{\lambda_m l_i}{d_i}\right). \quad (62)$$

Although this could be approximated using the leading eigenvalue, as done in Section 2, the expression is still complicated and does not provide further insight to the multilayer critical time behaviour. However, the critical time can be calculated numerically using Eq. (61), and is denoted 'Num.' in later analysis.

The analytical solutions given by Eqs. (17) and (56) were verified for multiple scenarios against two different numerical solutions to Eq. (1). The first scheme used finite differences, explained in Appendix A.2, and was implemented in MATLAB [33]. The second uses the commercial finite elements package FLEXPDE [34]. Agreement between the two numerical schemes and the analytical solutions were found to within expected numerical accuracy.

4. Numerical results

To explore the behaviour of the multilayer critical time a biperiodic region is considered, with $n/2$ repeating layers with 'A' and 'B' properties such as layer width, l_A and l_B, and diffusivity, D_A and D_B. That is, there are n layers in total with repeated layers $ABAB\ldots AB$, denoted in shorthand by $[A,B]$ or equivalently $[D_A, D_B]$. The region is defined with $x_0 = 0$ and $x_n = 1$, hence $L = 1$. For simplicity here, equal widths for both layers are used, so $l_i = 1/n$, but in general this is not necessary. Different diffusivities are used in each layer, where the larger diffusivity $D = 1$ and the smaller diffusivity $D = 0.1$. For simplicity, we let the conductivity parameters $\rho_i c_i = 1$ and the contact resistance $H_i = 20$, for all layers. The initial condition used is $f_i(x) = 0$ and the proportion of the steady state is $\alpha = 0.4627$.

Constant boundary conditions are used for Fig. 4, where $a_1 = 1 = a_2$ and $b_1 = 0 = b_2, \theta_1 = 1$ and $\theta_2 = 0$. Three different scenarios are presented in Fig. 4 for the critical time as a function of the number of repeated layers, $n/2$. The first scenario uses [1, 0.1] periodic layers, and the second scenario uses [0.1, 1]. The third 'Single D_{av}' scenario averages the diffusivities using Eq. (26), and calculates the critical time for the single layer solution, Eq. (20). Of interest is the convergence of the 'Num. [1, 0.1]' and 'Num. [0.1, 1]' scenarios from different sides of the averaged solution and the local maxima for the 'Num. [0.1, 1]' scenario. The case where $\alpha = 0.8435$ is not explored here as it is considered in Part 2 [31], where similar behaviour is also found.

Similar scenarios are explored in Fig. 5, but for different boundary conditions. The boundary condition at $x = x_0$ is made constant, with $a_1 = 1, b_1 = 0$ and $\theta_1 = 1$, and the boundary condition at $x = x_n$ is insulated, with $a_2 = 0, b_2 = 1$ and $\theta_2 = 0$. Both the 'Num. [1, 0.1]' and 'Num. [0.1, 1]' scenarios are symmetric about the 'Single D_{av}' scenario for Fig. 5. Note the 'Num. [0.1, 1]' solution does not give a local maximum as in Fig. 4. Since $\alpha = 0.4627$, this result is directly comparable with Eq. (3) using Eq. (26).

Both Figs. 4 and 5 demonstrate that a relatively large number of layers are required for accurate results when using the traditional averaging approach, Eq. (26). In particular, the averaging method has an error of approximately 10% for 10 repeated layers, or 20 layers in total. However, the error can be as high as 50% for two layers. The magnitude of this error is discussed in more detail in the companion paper [31], which uses a perturbation solution to find an expression for this critical time, and hence the magnitude of the error as a function of the number of layers and the diffusivities. The effect of varying diffusivities is discussed in the companion paper [31], for the simpler case of perfect contact between layers. There it is shown that as $D_A \to D_B$ the numerical critical time approaches the approximation, Eq. (3). For the parameters chosen here, the difference between the numerical and approximate critical times can be as much as 50%, naturally decreasing as the number of layers is increased.

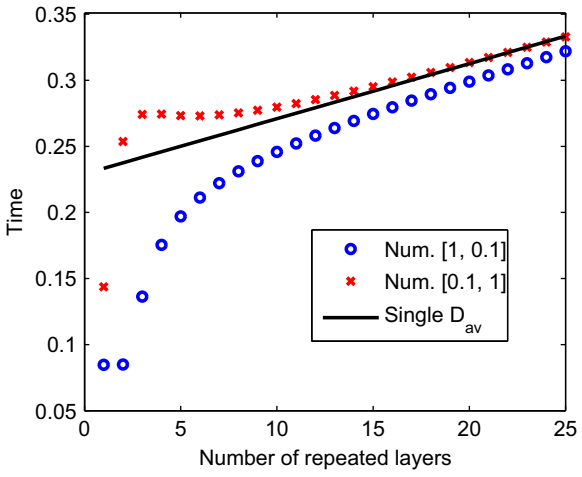

Fig. 4. Critical time versus number of repeated layers for a multilayer medium. Results are calculated numerically using Eq. (61) with the first 20 terms. Here $L = 1, l_i = 1/n, \alpha = 0.4627, a_1 = 1, b_1 = 0, \theta_1 = 1, a_2 = 0, b_2 = 1, \theta_2 = 0, f_i = 0$ and $H_i = 20$. Diffusivities are either [1, 0.1] or [0.1, 1]. 'Single D_{av}' uses the second single layer critical time, Eq. (21), with $D_{av} = 0.12$ from Eq. (26).

Previous work [14] demonstrated the limitations of the averaging approach using Eq. (4), for specific boundary conditions (as per Fig. 5) and using a different definition of critical time, where $U_n(x_n, t_c) = U_c$.

The main effect of imperfect contact on these results is the converging critical time having a positive slope. As the contact resistance, H_i, decreases the slope of the averaged solution increases. Hence as $H_i \to \infty$, the slope becomes zero, limiting to the case of perfect contact shown in Part 2 [31].

Although the numerical implementations provide some insight as to how the behaviour differs for multiple layers as opposed to a single layer, it fails to explain why this difference occurs. Hence in Hickson et al. [31] we explore an approximate perturbation of the exact solution which will illuminate this behaviour, and explain the local maximum found in the 'Num. [0.1, 1]' scenario in Fig. 4.

5. Discussion and conclusion

The most interesting point illustrated with this work is that layered materials do not exhibit symmetric properties. That is, the time taken to diffuse depends greatly on which order the materials are layered. Hence this work can be used to consider the inverse problem, where it is possible to apply the critical time to determine the individual properties of the layered materials. That is, two measurements of critical time, with the material direction switched, are sufficient to determine the properties of each individual layer. For example a possible experimental set up would involve raising the temperature of the material at $x = x_0$ with a thermocouple at $x = x_n$, and then reversing the experiment such that the temperature is raised at $x = x_n$ and the thermocouple placed at $x = x_0$.

Although only one definition for critical time has been explored here, it is possible to apply the exact solutions found to alternative definitions. Previous work [14] explored the effect of the temperature threshold on the critical time behaviour for an insulated boundary at $x = x_n$ and perfect contact. This work showed the same nonsymmetric behaviour as found here for the more general definition. The method used to find the exact solutions is extendable to cylindrical and spherical coordinates.

In summary, exact solutions were found for multilayer diffusion, with general boundary and interface conditions. These solutions were then used to numerically demonstrate the limitations of the traditional averaging methods, Eqs. (3) and (26). We demonstrated the symmetric convergence behaviour of critical time with number of layers and the differences caused by the layer order.

Appendix A

A.1. Proof of orthogonality condition

The orthogonality condition for n-layers is proven here for perfect contact using standard Sturm–Liouville theory. The original eigenfunction equation, which results from the separation of Eq. (40), is

$$\frac{\partial^2 X_{i,m}}{\partial x^2} = \frac{\varphi_m}{D_i} X_{i,m}, \quad i \in [1, n], \tag{63}$$

for the ith layer and mth eigenvalue, where $\varphi_m = -\lambda_m^2$. Multiplying both sides of Eq. (63) by $X_{i,p}$, for the pth eigenvalue where $m \neq p$, and integrating gives

$$\int_{x_{i-1}}^{x_i} X_{i,p} X''_{i,m} dx = \frac{\varphi_m}{D_i} \int_{x_{i-1}}^{x_i} X_{i,p} X_{i,m} dx \tag{64}$$

and similarly, for the other eigenvalue,

$$\int_{x_{i-1}}^{x_i} X_{i,m} X''_{i,p} dx = \frac{\varphi_p}{D_i} \int_{x_{i-1}}^{x_i} X_{i,m} X_{i,p} dx. \tag{65}$$

Subtracting Eq. (65) from Eq. (64), using integration by parts and simplifying gives

$$\begin{aligned}(\varphi_m - \varphi_p) \int_{x_{i-1}}^{x_i} X_{i,m} X_{i,p} dx &= D_i \left(\left[X_{i,p} X'_{i,m} \right]_{x_{i-1}}^{x_i} - \left[X_{i,m} X'_{i,p} \right]_{x_{i-1}}^{x_i} \right) \\ &= D_i \Big[X_{i,p}(x_i) X'_{i,m}(x_i) - X_{i,p}(x_{i-1}) X'_{i,m}(x_{i-1}) \\ &\quad - X_{i,m}(x_i) X'_{i,p}(x_i) + X_{i,m}(x_{i-1}) X'_{i,p}(x_{i-1}) \Big]. \end{aligned} \tag{66}$$

The same is done for the '$i+1$'th layer,

$$\begin{aligned}&(\varphi_m - \varphi_p) \int_{x_i}^{x_{i+1}} X_{i+1,m} X_{i+1,p} dx \\ &= D_{i+1} \Big[X_{i+1,p}(x_{i+1}) X'_{i+1,m}(x_{i+1}) - X_{i+1,p}(x_i) X'_{i+1,m}(x_i) \\ &\quad - X_{i+1,m}(x_{i+1}) X'_{i+1,p}(x_{i+1}) + X_{i+1,m}(x_i) X'_{i+1,p}(x_i) \Big]. \end{aligned} \tag{67}$$

The interface conditions are

$$X_{i,m}(x_i) = X_{i+1,m}(x_i), \tag{68}$$

$$\frac{r_i}{r_{i+1}} D_i \frac{\partial X_{i,m}}{\partial x}\bigg|_{x_i} = D_{i+1} \frac{\partial X_{i+1,m}}{\partial x}\bigg|_{x_i}, \tag{69}$$

for $i \in [1, n-1]$ where $r_i = \rho_i c_i$,. Using these, Eq. (67) becomes

$$\begin{aligned}&(\varphi_m - \varphi_p) \int_{x_i}^{x_{i+1}} X_{i+1,m} X_{i+1,p} dx \\ &= D_{i+1} X_{i+1,p}(x_{i+1}) X'_{i+1,m}(x_{i+1}) - \frac{r_i}{r_{i+1}} D_i X_{i,p}(x_i) X'_{i,m}(x_i) \\ &\quad - D_{i+1} X_{i+1,m}(x_{i+1}) X'_{i+1,p}(x_{i+1}) + \frac{r_i}{r_{i+1}} D_i X_{i,m}(x_i) X'_{i,p}(x_i). \end{aligned} \tag{70}$$

Adding r_i times Eq. (66) and r_{i+1} times Eq. (70) then gives

$$\begin{aligned}&(\varphi_m - \varphi_p) \left[r_i \int_{x_{i-1}}^{x_i} X_{i,m} X_{i,p} dx + r_{i+1} \int_{x_i}^{x_{i+1}} X_{i+1,m} X_{i+1,p} dx \right] \\ &= r_i D_i \Big[X_{i,m}(x_{i-1}) X'_{i,p}(x_{i-1}) - X_{i,p}(x_{i-1}) X'_{i,m}(x_{i-1}) \Big] \\ &\quad + r_{i+1} D_{i+1} \Big[X_{i+1,p}(x_{i+1}) X'_{i+1,m}(x_{i+1}) - X_{i,m}(x_{i+1}) X'_{i,p}(x_{i+1}) \Big]. \end{aligned}$$

Therefore the middle, x_i, points are always going to cancel out, leaving only the end points, $x = x_0$ and $x = x_n$. That is,

$$\begin{aligned}&(\varphi_m - \varphi_p) \sum_{i=1}^{n} r_i \int_{x_{i-1}}^{x_i} X_{i,m} X_{i,p} dx \\ &= r_1 D_1 [X_{1,m}(x_0) X'_{1,p}(x_0) - X_{1,p}(x_0) X'_{1,m}(x_0)] \\ &\quad + r_n D_n \Big[X_{n,p}(x_n) X'_{n,m}(x_n) - X_{n,m}(x_n) X'_{n,p}(x_n) \Big]. \end{aligned} \tag{71}$$

Given general boundary conditions at $x = x_0$:

$$\begin{aligned} a_1 X_{1,m}(x_0) + b_1 X'_{1,m}(x_0) &= 0 \\ a_1 X_{1,p}(x_0) + b_1 X'_{1,p}(x_0) &= 0 \end{aligned} \tag{72}$$

then for a_1 and b_1 both non-zero this requires the determinant

$$X_{1,m}(x_0) X'_{1,p}(x_0) - X_{1,p}(x_0) X'_{1,m} = 0 \tag{73}$$

and similarly at $x = x_n$. Hence Eq. (71) becomes

$$(\varphi_m - \varphi_p) \sum_{i=1}^{n} r_i \int_{x_{i-1}}^{x_i} X_{i,m} X_{i,p} dx = 0.$$

When $\varphi_m \neq \varphi_p$,

$$\sum_{i=1}^{n} r_i \int_{x_{i-1}}^{x_i} X_{i,m} X_{i,p} dx = 0$$

and hence the orthogonality condition has been proven.

This proof is extendable to the jump interface conditions, Eq. (23), although with more complicated algebra.

A.2. Finite difference scheme for layers

This explicit finite difference scheme uses second order central differences with an Euler time step. An added complexity arises from the layered nature of the problem. Fig. 6 depicts an interface between layers with nomenclature and indexing. The inner points of a layer use the standard first order time and second order space finite differencing, that is

$$\frac{\partial U_{j-1}}{\partial t} = \frac{D_i}{\Delta x^2}[U_{j-2} - 2U_{j-1} + U_j], \tag{74}$$

where U_j is the temperature at the spatial point j in layer i. The point on the interface is found using the flux matching condition, Eq. (25), as

$$\frac{\partial U_j}{\partial t} = \frac{1}{\Delta x^2}[D_i U_{j-1} - (D_i + D_{i+1})U_j + D_{i+1}U_{j+1}] \tag{75}$$

where U_j lies on the intersection of the i and $(i+1)$ layers, as shown in Fig. 6. Thus the differencing for this system can be illustrated by the following matrix

$$\frac{d}{dt}\begin{bmatrix} \vdots \\ U_{j-2} \\ U_{j-1} \\ U_j \\ U_{j+1} \\ U_{j+2} \\ \vdots \end{bmatrix} = \begin{bmatrix} \ddots & & & & & & \\ & \ddots & & & & & \\ \cdots & \chi_i & -2\chi_i & \chi_i & 0 & 0 & \cdots \\ \cdots & 0 & \chi_i & -\chi_i - \chi_{i+1} & \chi_{i+1} & 0 & \cdots \\ \cdots & 0 & 0 & \chi_{i+1} & -2\chi_{i+1} & \chi_{i+1} & \cdots \\ & & & & \ddots & & \\ & & & & & \ddots & \end{bmatrix} \begin{bmatrix} \vdots \\ U_{j-2} \\ U_{j-1} \\ U_j \\ U_{j+1} \\ U_{j+2} \\ \vdots \end{bmatrix}, \tag{76}$$

where $\chi_i = D_i/\Delta x$, and $\chi_{i+1} = D_{i+1}/\Delta x$. This is easily extended to multiple layers with numerous internal points and general boundary conditions. This can then be iterated in time using standard Euler time steps.

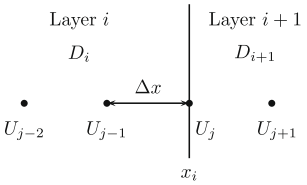

Fig. 6. Finite difference scheme indexing where i denotes the layer and j denotes the spatial discretisation.

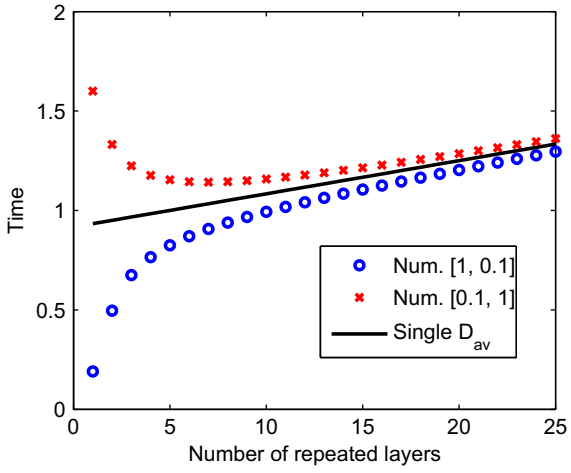

Fig. 5. Critical time versus number of repeated layers for a multilayer medium. Results are calculated numerically using Eq. (61) with the first 20 terms. Here $L = 1, l_i = 1/n, \alpha = 0.4627, a_1 = 1,\ b_1 = 0, \theta_1 = 1, a_2 = 1, b_2 = 0, \theta_2 = 0, f_i = 0$ and $H_i = 20$. Diffusivities are either [1, 0.1] or [0.1, 1]. 'Single D_{av}' uses the single layer critical time, Eq. (20), with $D_{av} = 0.12$ from Eq. (26).

References

[1] S.I. Barry, W.L. Sweatman, Modelling heat transfer in steel coils, ANZIAM J. (E) 50 (2009) C668.
[2] M. McGuinness, W.L. Sweatman, D.Y. Baowan, S.I. Barry, Annealing steel coils, in: T. Marchant, M. Edwards, G.N. Mercer (Eds.), MISG 2008 Proceedings, 2009.
[3] W.Y.D. Yuen, Transient temperature distribution in a multilayer medium subject to radiative surface cooling, Appl. Math. Model. 18 (1994) 93–100.
[4] N.M. Aguirre, G.G. De La Cruz, Y.G. Gurevich, G.N. Logvinov, M.N. Kasyanchuk, Heat diffusion in two-layer structures: photoacoustic experiments, Phys. Status Solidi B 220 (2000) 781–787.
[5] J. Diard, N. Glandut, C. Montella, J. Sanchez, One layer, two layers, etc. An introduction to the EIS study of multilayer electrodes. Part 1: Theory, J. Electroanal. Chem. 578 (2005) 247–257.
[6] V. Freger, Diffusion impedance and equivalent circuit of a multilayer film, Electrochem. Commun. 7 (2005) 957–961.
[7] P. Grossel, F. Depasse, Alternating heat diffusion in thermophysical depth profiles: multilayer and continuous descriptions, J. Phys. D: Appl. Phys. 31 (1998) 216–223.
[8] G. Pontrelli, F. de Monte, Mass diffusion through two-layer porous media: an application to the drug-eluting stent, Int. J. Heat Mass Transfer 50 (2007) 3658–3669.
[9] F. Martelli, A. Sassaroli, S. Del Bianco, G. Zaccanti, Solution of the time-dependent diffusion equation for a three-layer medium: application to study photon migration through a simplified adult head model, Phy. Med. Biol. 52 (2007) 2827–2843.
[10] S.H. Gilbert, R.T. Mathias, Analysis of diffusion delay in a layered medium, Biophys. J. 54 (1988) 603–610.
[11] F. de Monte, Transient heat conduction in one-dimension composite slab. A natural analytic approach, Int. J. Heat Mass Transfer 43 (2000) 3607–3619.
[12] G. Oturanc, A.Z. Sahin, Eigenvalue analysis of temperature distribution in composite walls, Int. J. Energ. Res. 25 (2001) 1189–1196.
[13] M. Fukuda, H. Kawai, Diffusion of low molecular weight substances into a laminar film. 1: Rigorous solution of the diffusion equations in a composite film of multiple layers, Polym. Eng. Sci. POLYM ENG SCI 35 (8) (1995) 709–721.
[14] R.I. Hickson, S.I. Barry, G.N. Mercer, Exact and numerical solutions for effective diffusivity and time lag through multiple layers, ANZIAM J. (E) 50 (2009) C682–C695.
[15] J.R. Miller, P.M. Weaver, Temperature profiles in composite plates subject to time-dependent complex boundary conditions, Compos. Struct. 59 (2003) 267–278.
[16] F. de Monte, An analytic approach to the unsteady heat conduction processes in one-dimensional composite media, Int. J. Heat Mass Transfer 45 (2002) 1333–1343.
[17] Y. Sun, I.S. Wichman, On transient heat conduction in a one-dimensional composite slab, Int. J. Heat Mass Transfer 47 (2004) 1555–1559.
[18] M. Fukuda, H. Kawai, Diffusion of low molecular weight substances into a fibre with skin-core structure – rigorous solution of the diffusion equations in a coaxial cylinder of multiple components, Polym. Eng. Sci. 34 (4) (1994) 330–340.
[19] X. Lu, P. Tervola, M. Viljanen, Transient analytical solution to heat conduction in a composite circular cylinder, Int. J. Heat Mass Transfer 49 (2006) 341–348.
[20] M.F.A. Azeez, A.F. Vakakis, Axisymmetric transient solutions of the heat diffusion problem in layered composite media, Int. J. Heat Mass Transfer 43 (2000) 3883–3895.
[21] K. Landman, M. McGuinness, Mean action time for diffusive processes, J. Appl. Math. Decis. Sci. 4 (2) (2000) 125–141.
[22] A. McNabb, G.C. Wake, Heat conduction and finite measures for transition times between steady states, IMA J. Appl. Math. 47 (2) (1991) 192–206.
[23] A. McNabb, Mean action times, time lags and mean first passage times for some diffusion problems, Math. Comput. Model. 18 (10) (1993) 123–129.
[24] R. Ash, R.M. Barrer, D.G. Palmer, Diffusion in multiple laminates, Brit. J. Appl. Phys. 16 (1965) 873–884.
[25] R.M. Barrer, Diffusion and permeation in heterogenous media, in: J. Crank, G.S. Park (Eds.), Diffusion in Polymers, Academic Press, London, 1968, pp. 165–215.

[26] J. Crank, The Mathematics of Diffusion, Oxford University press, England, 1957.
[27] G.L. Graff, R.E. Williford, P.E. Burrows, Mechanisms of vapor permeation through multilayer barrier films: Lag time versus equilibrium permeation, J. Appl. Phys. 96 (4) (2004) 1840–1849.
[28] B. Kruczek, H.L. Frisch, R. Chapanian, Analytical solution for the effective time lag of a membrane in a permeate tube collector in which Knudsen flow regime exists, J. Membrane Sci. 256 (2005) 57–63.
[29] J. Absi, D.S. Smith, B. Nait-Ali, S. Granjean, J. Berjonnaux, Thermal response of two-layer systems: numerical simulation and experimental verification, J. Eur. Ceram. Soc. 25 (2005) 367–373.
[30] R. Ash, R.M. Barrer, J.H. Petropoulos, Diffusion in heterogeneous media: properties of a laminated slab, Brit. J. Appl. Phys. 14 (1963) 854–862.
[31] R.I. Hickson, S.I. Barry, G.N. Mercer, Critical times in multilayer diffusion. Part 2: Approximate solutions, Int. J. Heat Mass Transfer 52 (2009) 5784–5791.
[32] H.S. Carslaw, J.C. Jaeger, Conduction of Heat in Solids, Clarendon Press, Oxford, 1959.
[33] MATLAB®, The MathWorks Inc., Natick, Massachusetts, <http://www.mathworks.com/products/matlab/>.
[34] FlexPDE, PDE Solutions Inc., Spokane Valley, <http://www.pdesolutions.com>.